Physica A 387 (2008) 6513–6525

Contents lists available at ScienceDirect

Physica A

journal homepage: www.elsevier.com/locate/physa

Critical behavior of long linear *k*-mers on honeycomb lattices

D.A. Matoz-Fernandez, D.H. Linares, A.J. Ramirez-Pastor *

Dpto. de Física, Instituto de Física Aplicada, Universidad Nacional de San Luis - CONICET, Chacabuco 917, 5700 San Luis, Argentina

ARTICLE INFO

Article history:
Received 23 April 2008
Received in revised form 10 July 2008
Available online 9 August 2008

PACS:
05.50.+q
64.70.Md
75.40.Mg

Keywords:
Lattice theory and statistics (Ising, Potts, etc.)
Transitions in liquid crystals
Numerical simulation studies

ABSTRACT

Monte Carlo (MC) simulations, finite-size scaling and theoretical analysis have been carried out to study the critical behavior of long linear particles of length k (k-mers) on honeycomb lattices. A nematic phase, characterized by a big domain of parallel k-mers, is separated from the isotropic state, by a continuous transition occurring at a finite density θ_c. Our study allowed: (1) to determine the minimum value of k ($k_{\min}$), which allows the formation of the nematic phase, being $k_{\min} = 11$; (2) to predict the dependence of θ_c on k, being $\theta_c(k) \propto k^{-1}$; and (3) to obtain the critical exponents, which indicate that the transition belongs to the 2D three-state Potts universality class.

1. Introduction

The study of the isotropic–nematic (I–N) phase transition in a system of long straight rigid rods on two-dimensional lattices has been tackled in three previous contributions referred to as I, II and III throughout this article [1–3]. In I, extensive Monte Carlo (MC) simulations supplemented by analysis, using finite-size scaling (FSS) theory were carried out to study the I–N phase transition in a system of long rigid rods deposited on square and triangular lattices. In the case of FSS analysis, the conventional normalized scaling variable $\epsilon \equiv T/T_c - 1$ was replaced by $\epsilon \equiv \theta/\theta_c - 1$, where T, T_c, θ and θ_c represent temperature, critical temperature, density and critical density, respectively. Based on the strong axial anisotropy of the nematic phase, an order parameter measuring the orientation of the particles was introduced. Taking advantage of its definition, we were able to study, for the first time, the universality class of the I–N phase transition occurring in the system. The accurate determination of critical exponents, along with the behavior of Binder cumulants, revealed that the transition belongs to the 2D Ising (three-state Potts) model universality class for square (triangular) lattices.

Later, in paper II, the I–N phase transition was analyzed in terms of configurational entropy. For this purpose, the configurational entropy of a system of straight rigid rods deposited on a square lattice was calculated by Monte Carlo (MC) simulations and thermodynamic integration method [4]. A comparison between the configurational entropy of the system and that corresponding to a fully aligned system (1) confirmed previous results in the literature [5], namely, the existence of a I–N phase transition at intermediate densities for long rods; (2) allowed us to estimate the minimum value of k, which leads to the formation of a nematic phase and provided an interesting interpretation of this critical value; (3) provided numerical evidence for the existence of a second phase transition (from a nematic to a non-nematic state) occurring at a density close to 1 and (4) allowed us to test the predictions of the main theoretical models developed to treat the polymer adsorption problem.

* Corresponding author.
E-mail address: antorami@unsl.edu.ar (A.J. Ramirez-Pastor).

0378-4371/$ – see front matter © 2008 Elsevier B.V. All rights reserved.
doi:10.1016/j.physa.2008.08.010

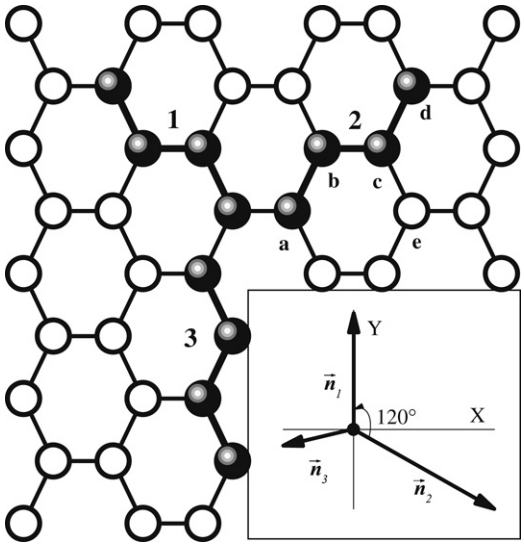

Fig. 1. Linear tetramers adsorbed on honeycomb lattices. Full and empty circles represent tetramer units and empty sites, respectively. Inset: Schematic representation of the set of vectors $\{\vec{n}_1, \vec{n}_2, \vec{n}_3\}$ for honeycomb lattices.

Paper III was a step further, analyzing the dependence of the critical density on the particle size k for square and triangular lattices. The results were obtained by combining Monte Carlo simulations, finite-size scaling techniques and theoretical analysis. The exhaustive study allowed us to determine the minimum value of $k(k_{\min} = 7)$, which allows the formation of a nematic phase on a triangular lattice. In addition, the critical density dependence on the particle size k was reported, being $\theta_c(k) \propto k^{-1}$.

I, II, and III, along with the seminal contribution of Ghosh and Dhar [5] have been limited to square and triangular lattices, where the concept of straight rigid rod is trivial. In this article, we consider the same lattice-gas model as that treated in I, II and II. Here, the difference is that we extend the analysis to honeycomb lattices, being that the adsorbate is a linear molecule of length k, maximizing the distance between first and last monomers in the chain. A complete study of the I–N phase transition occurring at intermediate densities was performed. Thus, the minimum value of k ($k_{\min}$), which allows the formation of the nematic phase, was determined; the dependence of θ_c on k was predicted; and the critical exponents were obtained. The results revealed that the transition belongs to the 2D three-state Potts universality class.

2. Model and basic definitions

In this section, the lattice-gas model for the adsorption of linear molecules is described. The surface is represented as an array of $M = L \times L$ adsorptive sites in a honeycomb lattice arrangement, where L denotes the linear size of the array. The linear molecule or (linear k-mer) is modeled as k interaction centers at a fixed separation, which is equal to the lattice constant a. However, in a honeycomb lattice, the geometry does not allow the existence of a straight rigid chain of monomers. In this case, we call linear k-mer to a array of adjacent monomers with the following sequence: once the first monomer is in place, the second monomer occupies one of the three nearest-neighbors of the first monomer. The third monomer occupies one of the two nearest-neighbors of the second monomer. i-esime monomer (for $i \geq 4$) occupies one of the two nearest-neighbors of the preceding monomer, which maximizes the distance between first monomer and i-esime monomer. This procedure allow us to place k monomers on a honeycomb lattice without creating an overlap. As an example, Fig. 1 shows a available configuration for a linear tetramer adsorbed on a honeycomb lattice. Once first, second and third monomers were adsorbed in positions denoted as a, b and c, respectively, there exist two possible positions for adsorbing fourth monomer, d and e. In order to maximize the distance between the position of first and fourth monomers, site d is selected and site e is discarded. The only interaction between different ad-molecules is hard-core exclusion: no site can be occupied by more than one k-mer. The surface coverage (or density) is defined as $\theta = kN/M$, where N is the number of adsorbed k-mers.

In order to follow the formation of the nematic phase from the isotropic phase, we need a related order parameter. To this end, we use the order parameter defined in I, which in this case can be written as

$$\delta = \frac{\left|\vec{n}_1 + \vec{n}_2 + \vec{n}_3\right|}{\left|\vec{n}_1\right| + \left|\vec{n}_2\right| + \left|\vec{n}_3\right|} \tag{1}$$

where each vector $\vec{n}_m$ is associated to one of the 3 possible orientations (or directions) for a k-mer on the lattice (see k-mers marked with 1, 2 and 3 in Fig. 1). In addition, (1) the $\vec{n}_i$'s lie in the same plane (or are co-planar) and point radially outward from a given point P which is defined as coordinate origin; (2) the angle between two consecutive vectors, $\vec{n}_i$ and $\vec{n}_{i+1}$, is

equal to $2\pi/3$; and (3) the magnitude of $\vec{n}_i$ is equal to the number of k-mers aligned along the i-direction (see inset in Fig. 1). Note that the $\vec{n}_i$'s have the same directions as the q vectors in Ref. [6]. These directions are not coincident with the allowed directions for the k-mers on the real lattice.

The problem has been studied by grand canonical MC simulations, using a typical adsorption-desorption algorithm [7–10]. The procedure is as follows. Once the value of the chemical potential μ is set, a linear k-uple of nearest-neighbor sites is chosen at random. Then, if the k sites are empty, an attempt is made to deposit a k-mer with probability $W = \min\{1, \exp(\mu/k_BT)\}$, where k_B is the Boltzmann constant and T is the temperature; if the k sites are occupied by units belonging to the same k-mer, an attempt is made to desorb this k-mer with probability $W = \min\{1, \exp(-\mu/k_BT)\}$; and otherwise, the attempt is rejected. In addition, displacement (diffusional relaxation) of adparticles to nearest-neighbor positions, by either jumps along the k-mer axis or reptation by rotation around the k-mer end, must be allowed in order to reach equilibrium in a reasonable time. An MC step (MCs) is achieved when M k-uples of sites have been tested to change its occupancy state. Typically, the equilibrium state can be well reproduced after discarding the first $r' = 10^6$ MCs. Then, the next $r = 3 \times 10^6$ MCs are used to compute averages.

In our Monte Carlo simulations, we varied the chemical potential μ and monitored the density θ and the order parameter δ, which can be calculated as simple averages. The quantities related with the order parameter, such as the susceptibility χ, and the reduced fourth-order cumulant U_L introduced by Binder [4] were calculated as:

$$\chi = \frac{L^2}{k_BT}[\langle\delta^2\rangle - \langle\delta\rangle^2] \tag{2}$$

and

$$U_L = 1 - \frac{\langle\delta^4\rangle}{3\langle\delta^2\rangle^2}, \tag{3}$$

where $\langle\cdots\rangle$ means the average over the MC simulation runs and k_B is the Boltzmann constant.

Finally, the configurational entropy was calculated, by using MC simulations and thermodynamic integration method [11–14]. The method in the grand canonical ensemble relies upon integration of the chemical potential μ on coverage along a reversible path between an arbitrary reference state and the desired state of the system. This calculation also requires the knowledge of the total energy U for each obtained coverage. Thus, for a system made of N particles on M lattice sites, we have:

$$S(N, M, T) = S(N_0, M, T) + \frac{U(N, M, T) - U(N_0, M, T)}{T} - \frac{1}{T}\int_{N_0}^{N} \mu \mathrm{d}N'. \tag{4}$$

In our case $U(N, M, T) = 0$ and the determination of the entropy in the reference state, $S(N_0, M, T)$, is trivial [$S(N_0, M, T) = 0$ for $N_0 = 0$]. Note that the reference state, $N \to 0$, is obtained for $\mu/k_BT \to -\infty$. Then,

$$\frac{s(\theta, T)}{k_B} = -\frac{1}{k_BT}\int_0^{\theta} \frac{\mu}{k}\mathrm{d}\theta' \tag{5}$$

where $s(= S/M)$ is the configurational entropy per site, $\theta(= kN/M)$ is the surface coverage (or density).

All calculations were carried out using the parallel cluster BACO of Universidad Nacional de San Luis, Argentina. This facility consists of 60 PCs each with a 3.0 GHz Pentium-4 processor.

3. Results

3.1. Determination of the minimum value of k which allows the formation of a nematic phase

As it was established in Ref. [5], the minimum value of k, which allows the formation of a nematic phase on a square lattice at intermediate densities, is $k_{\min} = 7$. Later, the results in III demonstrated that the value of $k_{\min}$ for triangular lattices coincides with that obtained for square lattices. This critical quantity has not been calculated yet for honeycomb lattices. Then, our first objective is to obtain $k_{\min}$ for such geometry. For this purpose, two criteria have been applied: (1) the behavior of the nematic order parameter δ as a function of coverage; and (2) a comparison between the configurational entropy of the system, obtained by MC simulations, and the corresponding to a fully aligned system (nematic phase), whose calculation reduces to the 1D case.

The results obtained in the first case are shown in Fig. 2. The figure presents the nematic order parameter δ as a function of coverage for $k = 10$, 11 and 12 and $L/k = 20$. For $k > 10$, δ presents the typical behavior of a orientational order parameter in the presence of a I–N phase transition. Thus, at low densities the system is disordered, all orientations are equivalents and δ tends to zero. As the density is increased, the k-mers align along one direction, and δ is different from zero. On the other hand, we did not find nematic order for $k \leq 10$. This finding is a clear indication that $k_{\min} = 11$ for honeycomb lattices.

As an independent corroboration of the results obtained in the last figure, Fig. 3 presents the study of the I–N phase transition from a new perspective, namely, a comparison between the configurational entropy of the system and that

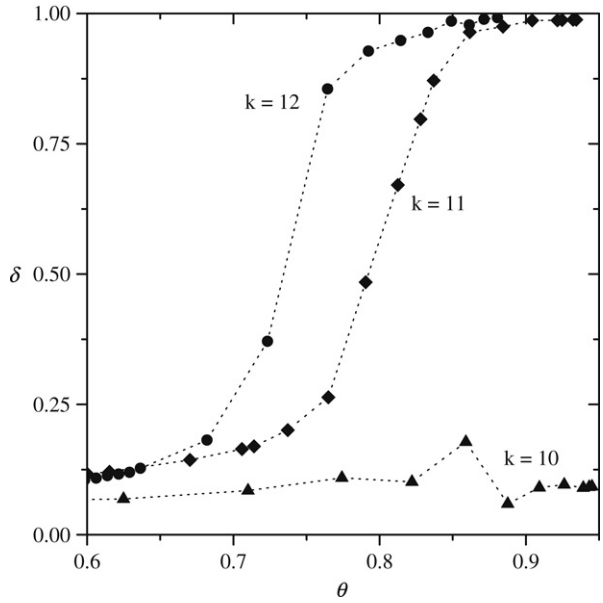

Fig. 2. Surface coverage dependence of the nematic order parameter for different k as indicated and $L/k = 20$.

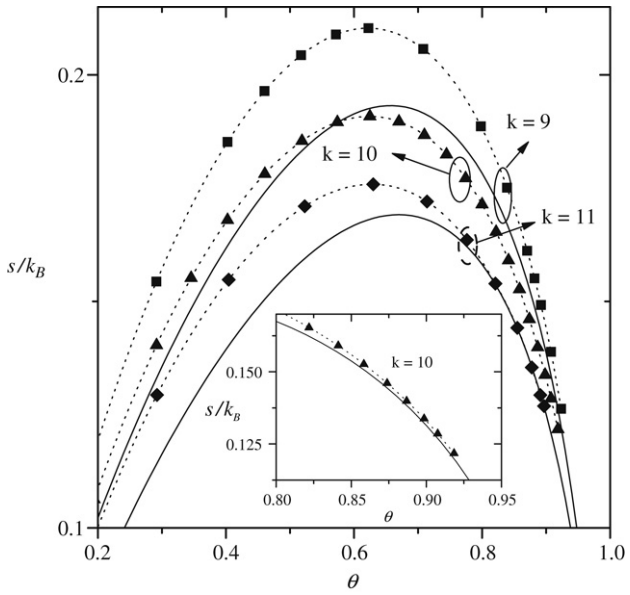

Fig. 3. Configurational entropy per site (in units of k_B) versus surface coverage for different k as indicated and $L/k = 20$. Dotted line and symbols represent MC results for honeycomb lattices, and solid lines correspond to exact results for one-dimensional systems.

corresponding to a fully aligned system. Dotted line and symbols represent MC results for triangular lattices, $k = 9$, 10 and 11 and $L/k = 20$. Calculation of $s(\theta)/k_B$ through Eq. (5) is straightforward and computationally simple, since the coverage dependence of μ/k_BT is evaluated following the standard procedure of MC simulation described in previous section. Then, $\mu(\theta)/k_BT$ is spline-fitted and numerically integrated. On the other hand, when the nematic phase is formed, the system is characterized by a big domain of parallel k-mers. The calculation of the entropy of this fully aligned state having density θ reduces to the calculation of a one-dimensional problem [15]

$$\frac{s(\theta)}{k_B} = \left[1 - \frac{(k-1)}{k}\theta\right] \ln\left[1 - \frac{(k-1)}{k}\theta\right] - \frac{\theta}{k} \ln \frac{\theta}{k} - (1-\theta) \ln (1-\theta)\,. \tag{6}$$

Results from Eq. (6) for $k = 9$, 10 and 11 are shown in Fig. 3 (solid lines). The inset shows the data for $k = 10$ and high densities. As it can be observed, for $k \leq 10$, the 1D results present a smaller s/k_B than the 2D simulation data over all the range of θ. For $k \geq 11$, there exists a range of coverage for which the difference between the 1D value and the true 2D value is

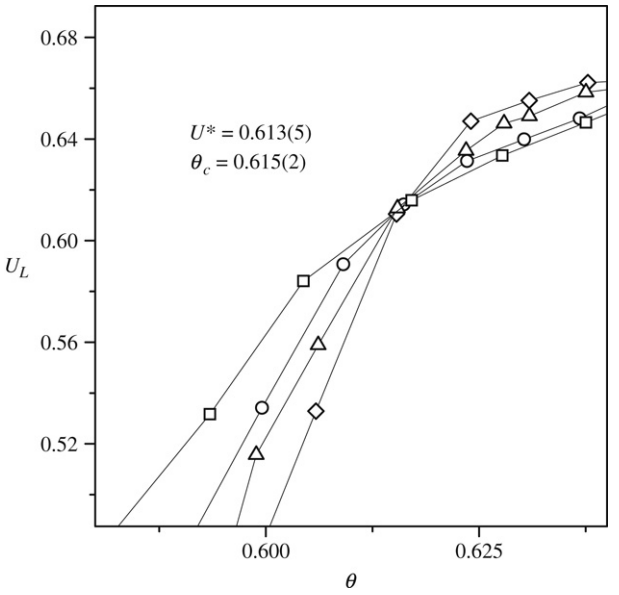

Fig. 4. Curves of U_L vs θ for honeycomb lattices, $k = 15$ and different lattice sizes as indicated. From their intersections one obtains θ_c.

very small. In other words, for $k \geq 11$ and intermediate densities, it is more favorable for the k-mers to align spontaneously, since the resulting loss of orientational entropy is by far compensated by the gain of translational entropy. The behavior of s confirms the existence of nematic order for $k \geq 11$.

3.2. Dependence of the critical density on the size of the k-mer

Once $k_{\min}$ has been established, we now discuss the behavior of the critical density as a function of the size k. In the case of the standard theory of finite-size scaling [4,16], when the phase transition is temperature driven, the technique allows for various efficient routes to estimate T_c from MC data. One of these methods, which will be used in this case, is from the temperature dependence of $U_L(T)$, which is independent of the system size for $T = T_c$. In other words, T_c is found from the intersection of the curve $U_L(T)$ for different values of L, since $U_L(T_c) = \text{const}$. In our study, we modified the conventional finite-size scaling analysis, by replacing temperature by density [1]. Under this condition, the critical density has been estimated from the plots of the reduced four-order cumulants $U_L(\theta)$ plotted versus θ for several lattice sizes. As an example, Fig. 4 shows the results for k-mers of size $k = 15$. In the case of the figure, the value obtained was $\theta_c = 0.615(2)$.

With respect to the value of the cumulant at the transition temperature, U^*, we obtained $U^* = 0.613(5)$. This value of U^* is practically indistinguishable from previous estimates for the two-dimensional three-state Potts model (see for instance Ref. [17], where $U^* \cong 0.613$). This finding may be taken as a first indication of universality. However, as recently pointed out by Selke et al. [18,19], the value of the cumulant intersection may depend on various details of the model, which do not affect the universality class, in particular, the boundary condition, the shape of the lattice, and the anisotropy of the interactions. Consequently, more research is required to determine the universality class of a phase. In this sense, a systematic analysis of critical exponents will be carried out in the next Section, where the fixed point value of the cumulants along with the critical exponents obtained by FSS will be considered to resolve the universality class of the I–N phase transition.

The procedure of Fig. 4 was repeated for $11 \leq k \leq 18$ and the results are collected in Fig. 5. The log–log plot shows that the critical density follows a power law as $\theta_c(k) \propto k^{-1}$. The understanding of the dependence of $\theta_c(k)$ on k can be developed by analyzing the delicate balance between the configurational entropy of an isotropic system and the corresponding to a fully aligned system. This will be discussed in the following.

The entropy of the fully aligned state having density θ can be obtained from Eq. (6). With respect to calculation of the configurational entropy of an isotropic system, two multisite-adsorption theories have been considered: the first is the well-known Guggenheim–DiMarzio approach [20,21] for rigid rod molecules and the second is the recently developed semiempirical model for adsorption of polyatomics [22]. Details on the derivation of these theories are given in Appendices A–C.

From a given value of k (which depends on the approximation considered), the 2D [Eqs. (27) and (48)] and 1D [Eq. (6)] curves cross at intermediate densities and two well differentiated regimes can be observed. In the first regime, which occurs at low densities, the 2D approaches predict a larger entropy than the 1D data. In the second regime (at high densities) the behavior is inverted and the 2D data present a smaller s/k_B than the 1D results. Given that the theoretical results in 2D assume isotropy in the adlayer (see Appendix A, where this point is explicitly considered), the crossing of the curves shows that, in the second regime, the contribution to the 2D entropy from the isotropic configurations is lower than the

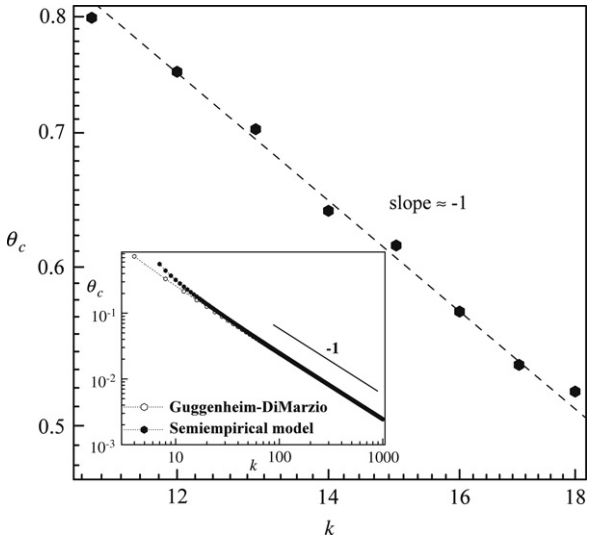

Fig. 5. Simulated and theoretical (inset) results for critical density θ_c as a function of k. The symbology is indicated in the figure.

contribution from the aligned states. Then, the existence of an intersection point is indicative of a I–N transition and allows us to estimate $k_{\min}$ and θ_c from the different approximations studied. This intersection point can be easily calculated through a standard computing procedure; in our case, we used MATHEMATICA software. The results are shown in the inset of Fig. 5. The symbology is indicated in the figure.

The excellent qualitative agreement between theoretical and simulation data provides a physical interpretation of the observed k dependence of the isotropic–nematic phase transition. Thus, at intermediate densities, it is more favorable for the k-mers to align spontaneously, since the resulting loss of orientational entropy is by far compensated by the gain of translational entropy. With respect to $k_{\min}$, the Guggenheim–DiMarzio approach predicts a value of $k_{\min}^{GD} = 4$. On the other hand, the semiempirical model performs better than the Guggenheim–DiMarzio approximation, predicting a value of $k_{\min}^{SE} = 7$. However, the determination of the "exact" value of $k_{\min} = 11$ from theoretical arguments is still an open problem.

3.3. Determination of the critical exponents for the I–N phase transition: Universality of the transition

We now analyze the critical exponents corresponding to the I–N phase transition of long linear k-mers on honeycomb lattices. In this case, there are three competing ordered states near the transition (or the order parameter has three components), and this transition is expected to be in the universality class of the two-dimensional Potts model with $q = 3$.

The critical behavior of the model has been investigated by means of the computational scheme described in the previous paragraphs, and finite-size scaling analysis. The FSS theory implies the following behavior of δ, χ and U_L at criticality:

$$\delta = L^{-\beta/\nu}\tilde{\delta}(L^{1/\nu}\epsilon), \tag{7}$$

$$\chi = L^{\gamma/\nu}\tilde{\chi}(L^{1/\nu}\epsilon) \tag{8}$$

and

$$U_L = \tilde{U}_L(L^{1/\nu}\epsilon), \tag{9}$$

for $L \to \infty, \epsilon \to 0$, such that $L^{1/\nu}\epsilon =$ finite, being $\epsilon \equiv T/T_c - 1$. Here β, γ and ν are the standard critical exponents of the order parameter ($\delta \sim -\epsilon^{\beta}$ for $\epsilon \to 0^-, L \to \infty$), susceptibility($\chi \sim |\epsilon|^{\gamma}$ for $\epsilon \to 0, L \to \infty$) and correlation length ξ ($\xi \sim |\epsilon|^{-\nu}$ for $\epsilon \to 0, L \to \infty$), respectively. $\tilde{\delta}$, $\tilde{\chi}$ and $\tilde{U}_L$ are scaling functions for the respective quantities.

As in the previous Section, we modified the standard FSS analysis by replacing temperature by density. Under this condition, $\epsilon \equiv \theta/\theta_c - 1$.

The calculations were developed for two k-mer sizes ($k = 15$ and $k = 18$). With these values of k, it is expected the existence of a nematic phase at intermediate densities. The effect of finite size was investigated by examining 15-mers (18-mers) on honeycomb lattices with $L = 90, 120, 150, 180$ ($L = 72, 108, 144, 180$), with an effort reaching almost the limits of our computational capabilities.

As stated in Refs. [23–25], the critical exponent ν can be obtained by considering the scaling behavior of certain thermodynamic derivatives with respect to the coverage, for example, the derivative of the cumulant and the logarithmic derivative of δ. In Fig. 6(a), we plot the maximum value of these derivatives as a function of system size on a log–log scale.

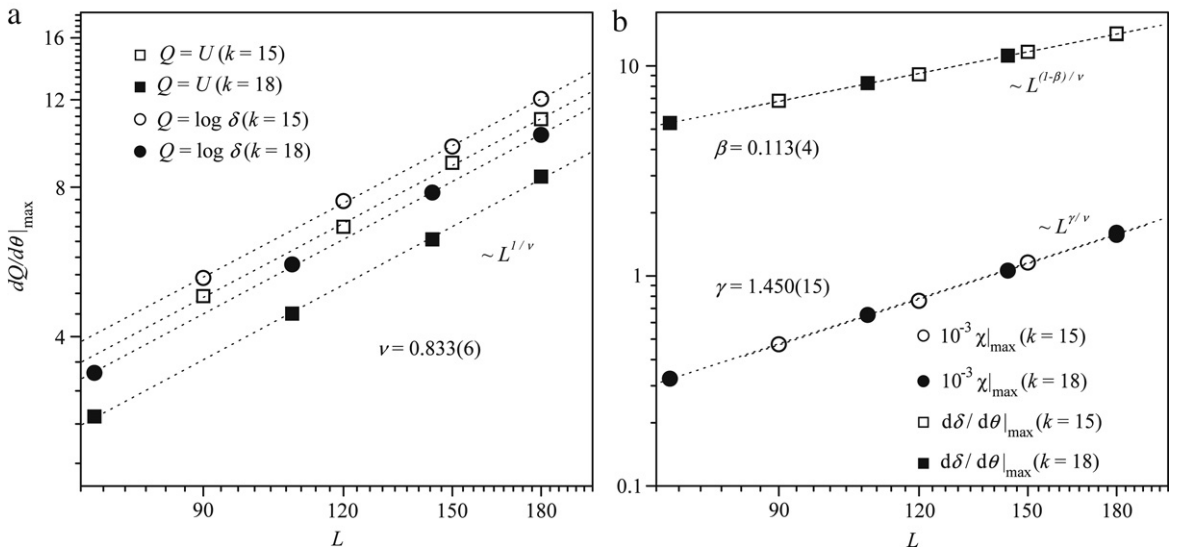

Fig. 6. (a) Log–log plot of the size dependence of the maximum values of derivatives of various thermodynamic quantities used to determine ν. (b) Log–log plot of the size dependence of the maximum value of the susceptibility and the maximum value of the derivative of the order parameter used to determine γ and β, respectively.

The results for $1/\nu$ from these fits are: $1/\nu^{(U;k=15)} = 1.198(30)$; $1/\nu^{(U;k=18)} = 1.210(18)$; $1/\nu^{(\log\delta;k=15)} = 1.194(15)$; and $1/\nu^{(\log\delta;k=18)} = 1.203(13)$. Combining these four estimates, we obtain $1/\nu = 1.201(8)$ or $\nu = 0.833(6)$.

Once we know ν, the critical exponent γ can be determined by scaling the maximum value of the susceptibility. Our data for $\chi|_{max}$ are shown in Fig. 6(b). The values obtained from the fits corresponding to $k = 15$ and $k = 18$ are $\gamma = 1.452(26)$ and $\gamma = 1.448(17)$, respectively. Combining the two estimates, we obtain the final value $\gamma = 1.450(15)$, which is indicated in the figure.

On the other hand, the standard way to extract the exponent β is to study the scaling behavior of δ at the point of inflection, i.e., at the point where $d\delta/d\theta$ is maximal. Since these points should scale as usual, we expect [23–25]

$$\left.\frac{d\delta}{d\theta}\right|_{max} \propto L^{(1-\beta)/\nu}. \tag{10}$$

The scaling of $d\delta/d\theta|_{max}$ is shown in Fig. 6(b). The linear fit through all data points gives $\beta = 0.112(4)$ for $k = 15$ and $\beta = 0.114(8)$ for $k = 18$. Combining the two estimates, we obtain the final value $\beta = 0.113(4)$, which is indicated in the figure.

We can thus conclude that our estimates of the exponents ν, β and γ are fully consistent with the universality class of the two-dimensional Potts model with $q = 3$ ($\nu = 5/6$, $\beta = 1/9$ and $\gamma = 13/9$). The scaling behavior can be further tested by plotting $\delta L^{\beta/\nu}$ vs $|\epsilon|L^{1/\nu}$, $\chi L^{-\gamma/\nu}$ vs $\epsilon L^{1/\nu}$ and U_L vs $|\epsilon|L^{1/\nu}$ and looking for data collapsing. As is shown in Figs. 7 and 8, the data scale extremely well using $\nu = 5/6$, $\beta = 1/9$ and $\gamma = 13/9$, which reinforces the robustness of the scaling results obtained here.

4. Conclusions

We have addressed the critical properties of long linear k-mers on honeycomb lattices. The results were obtained by using extensive MC simulations, FSS theory and theoretical analysis.

According to the present study the critical behavior of the system is characterized by the following properties:

(1) The minimum value of k, which allows the formation of a nematic phase on a honeycomb lattice is $k_{min} = 11$.
(2) The critical density dependence on the particle size follows a power law as $\theta_c(k) \propto k^{-1}$. As it was demonstrated from theoretical calculations, the delicate balance between the configurational entropy of an isotropic system and that corresponding to a fully aligned system (nematic phase) allows us to interpret this dependence of $\theta_c(k)$ on k.
(3) The evaluation of the fixed point of the cumulants along with the values of the critical exponents ν, β and γ clearly indicate that the observed I–N phase transition belongs to the universality class of the two-dimensional Potts model with $q = 3$.

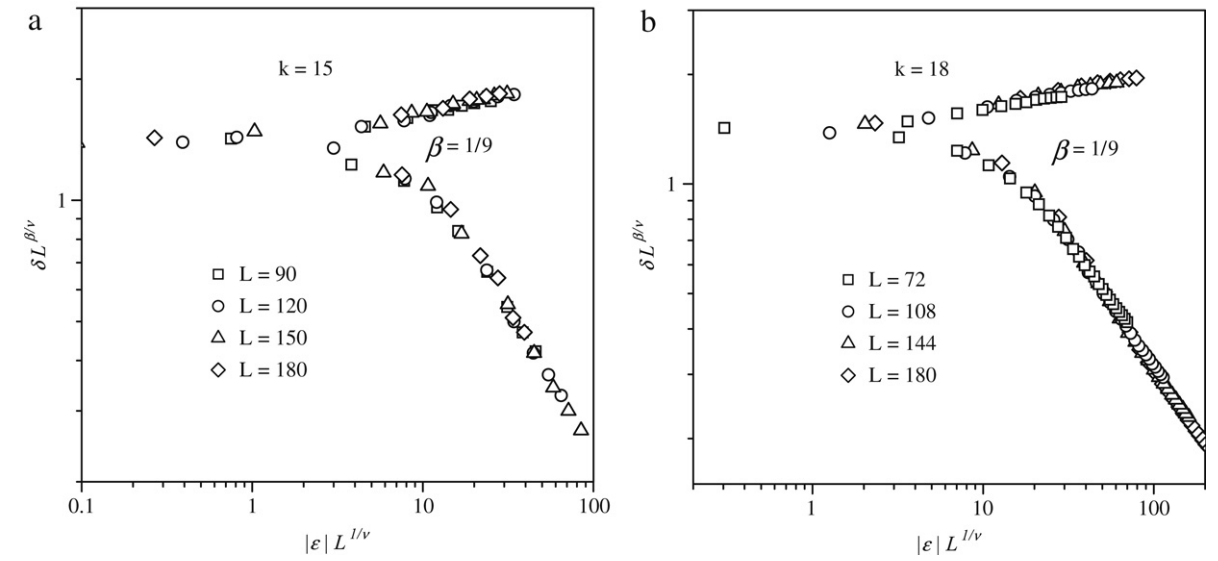

Fig. 7. (a) Data collapsing of the order parameter, $\delta L^{\beta/\nu}$ vs $|\epsilon|L^{1/\nu}$, for $k = 15$. The plot was made using the exact 2D three-state Potts model exponents $\nu = 5/6$ and $\beta = 1/9$. (b) As in part (a) for $k = 18$.

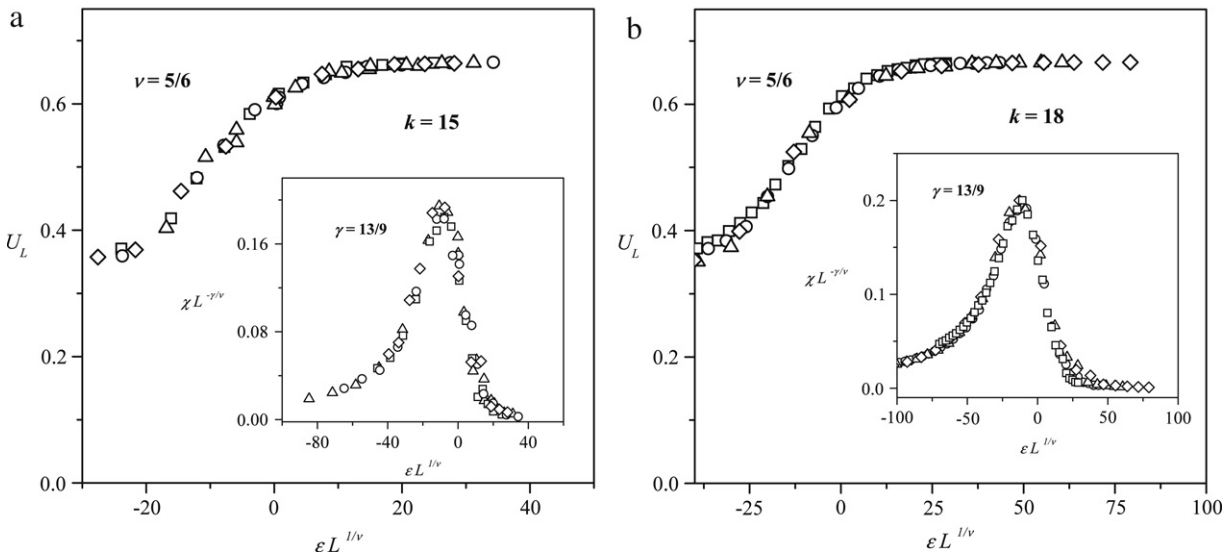

Fig. 8. (a) Data collapsing of the cumulant, U_L vs $\epsilon L^{1/\nu}$, and of the susceptibility, $\chi L^{-\gamma/\nu}$ vs $\epsilon L^{1/\nu}$ (inset), for $k = 15$. The plot was made using the exact 2D three-state Potts model exponents $\nu = 5/6$ and $\gamma = 13/9$. (b) As in part (a) for $k = 18$.

Acknowledgments

This work was supported in part by CONICET (Argentina) under project PIP 6294; Universidad Nacional de San Luis (Argentina) under project 322000 and the National Agency of Scientific and Technological Promotion (Argentina) under project 33328 PICT 2005.

Appendix A. Guggenheim–DiMarzio approximation

In 1944, Guggenheim proposed an interesting method to calculate the combinatory term in the canonical partition function [20]. Later, in a valuable contribution, DiMarzio obtained the Guggenheim's factor for a model of rigid rod molecules [21]. In this section we reproduce the calculations developed by DiMarzio, who obtained the number of ways to pack rigid rods onto a cubic lattice and its generalization to lattices of connectivity γ.

Let us place N straight rigid rods (linear k-mers) onto a cubic lattice. We will assume that only the three mutually perpendicular base vector directions are directions in which the rigid rods lie. The number of molecules that lie in the

direction i will be denoted by $N_i (i = 1, 2, 3)$. We ask for the number of ways, $\Omega(\{\cdots N_i \cdots\}, N_0)$ to pack the N molecules such that N_i of them lie in the direction i and there are N_0 holes. The advantage of allowing only those orientations for which the molecules fit exactly onto the lattice, is that for the case of an isotropic distribution the value of Ω reduces to the value obtained previously by Guggenheim [20].

Let us place N_1 molecules, one at a time, onto the lattice in orientation 1, and then the N_2 molecules, one at a time, in orientation 2 and then place the remaining N_3 molecules, one at a time, in orientation 3. In order to estimate the number of ways to place the $(j_1 + 1)$th molecule onto the lattice, given that j_1 molecules have already been placed, we must know the probability that k contiguous sites lying in this orientation are empty. Here the subscript reminds us that we are discussing type 1 molecules. Consider a contiguous pair of sites arbitrarily chosen except for the fact that the line determined by the centers of these sites lies along orientation 1. Label the sites A and B. Site A has a probability of being empty equal to the fraction of sites that are unoccupied by molecular segments since site A can be thought of as chosen arbitrarily. If site A is empty, the ratio of the number of times it adjoins a polymer to the number of times it adjoins a vacant site is $2j_1/2(M - kj_1)$, where M is the total number of sites in the lattice. Notice that in writing this expression for the ratio, we counted only those pairs of contiguous sites which lie along orientation 1. The pairs which lie along orientations 2 and 3 are of no consequence as far as the nearest-neighbor statistics along orientation 1 are concerned.

The above ratio is also the ratio of the number of times a polymer adjoins site A (presumed empty) to the number of times a vacant site adjoins site A. Thus the probability that site B is empty given that site A is empty is

$$\frac{2(M - kj_1)}{2(M + kj_1) + 2j_1}. \tag{11}$$

We see that ν_{j_1+1}, the number of ways to place the $(j_1 + 1)$th molecule onto the lattice, is

$$\nu_{j_1+1} = (M - kj_1)\left[\frac{2(M - kj_1)}{2(M + kj_1) + 2j_1}\right]^{k-1}. \tag{12}$$

The total number of ways to place N_1 indistinguishable molecules onto the lattice in this orientation is

$$\frac{\prod_{j_1=0}^{N_1-1} \nu_{j_1+1}}{(N_1)!} = \frac{M!\,(M - kN_1 + N_1)!}{(M - kN_1)!M!\,(N_1)!} = \frac{(M - kN_1 + N_1)!}{(M - kN_1)!\,(N_1)!}. \tag{13}$$

Note that this result so far is equal to the exact number. That is to say, the number of ways to pack the molecules is the number of ways to arrange N_1 linear molecules and N_0 holes on a linear lattice (see Eq. (32)).

In order to count the number of ways to pack the N_2 molecules in the second orientation, given that we have already placed the N_1 molecules, we need to know the statistics for those pairs of neighboring sites whose centers are connected by a line in this direction. The number of these kind of nearest-neighbors to polymer molecules is $2kN_1 + 2j_2$ where j_2 is the number of polymer molecules in the second orientation and the number of these kind of nearest-neighbors to holes is $2M - (2kN_1 + 2kj_2)$.

The first segment of the $(j_2 + 1)$th molecule can go into the lattice in $(M - kN_1 - kN_2)$ places. The expectancy that a site is unoccupied when it is known that the adjacent site in the direction in which the molecules lies is unoccupied is

$$\frac{2(M - kN_1 - kj_2)}{2(M - kN_1 - kj_2) + 2(kN_1 + j_2)}. \tag{14}$$

We therefore have for ν_{j_2+1}

$$\nu_{j_2+1} = (M - kN_1 - kj_2)\left[\frac{(M - kN_1 - kj_2)}{(M - kN_1 - kj_2) + (kN_1 + j_2)}\right]^{k-1}. \tag{15}$$

The total number of ways to pack these indistinguishable molecules is

$$\frac{\prod_{j_2=0}^{N_2-1} \nu_{j_2+1}}{(N_2)!} = \frac{(M - kN_1)!\,(M - kN_2 + N_2)!}{(M - kN_1 - kN_2)!M!\,(N_2)!}. \tag{16}$$

By an exactly analogous reasoning process we obtain for ν_{j_3+1},

$$\nu_{j_3+1} = (M - kN_1 - kN_2 - kj_3)\left[\frac{(M - kN_1 - kN_2 - kj_3)}{(M - kN_1 - kN_2 - kj_3) + (kN_1 + kN_2 + j_3)}\right]^{k-1}, \tag{17}$$

$$\frac{\prod_{j_3=0}^{N_3-1} \nu_{j_3+1}}{(N_3)!} = \frac{(M - kN_1 - kN_2)!\,(M - kN_3 + N_3)!}{(M - kN_1 - kN_2 - kN_3)!M!\,(N_3)!}. \tag{18}$$

The product obtained from Eqs. (13), (16) and (18) gives the total number of ways to pack the molecules

$$\Omega(N_0, N_1, N_2, N_3) = \frac{(M - kN_1 + N_1)!}{(M - kN_1)!\,(N_1)!}\frac{(M - kN_1)!\,(M - kN_2 + N_2)!}{(M - kN_1 - kN_2)!M!\,(N_2)!}\frac{(M - kN_1 - kN_2)!\,(M - kN_3 + N_3)!}{(M - kN_1 - kN_2 - kN_3)!M!\,(N_3)!}$$
$$= \frac{\prod_{j=1}^{3}[M - (k-1)\,N_i]!}{(N_0)!\prod_{i=1}^{3}(N_i)!\,(M!)^2}. \tag{19}$$

As remarked before, this expression is exact when all the molecules are in one direction. Eq. (19) has the proper symmetry requirements. It is invariant under the permutation of the N_i. For the case $N_1 = N_2 = N_3 = N/3$ we obtain

$$\Omega = \frac{\{[N_0 + (2kN/3) + (N/3)]!\}^3}{N_0!\,[(N/3)!]^3\,(M!)^2}. \tag{20}$$

Eq. (19) can be generalized for a lattice of connectivity γ. If ones uses a mole fraction for molecules that are parallel with one another and a volume fraction for molecules that are perpendicular (it is assumed that the base vectors of the new space are orthogonal) then the appropriate generalization of Eq. (19) is

$$\Omega(N_0, \{N_i\}) = \frac{\prod_{i=1}^{\gamma/2}[M - (k-1)\,N_i]!}{(N_0)!\prod_{i=1}^{\gamma/2}(N_i)!\,(M!)^{\gamma/2-1}}, \tag{21}$$

where $\gamma/2$ is the dimensionality of the space. Again, if we allow $N_i = (2/\gamma)N$ (and $N_0 = M - kN$) then Eq. (19) reduces to the well-known Guggenheim's factor

$$\Omega(M, N, \gamma) = \left(\frac{\gamma}{2}\right)^N \frac{M!}{N!(M - kN)!}\left[\frac{\{M - kN + [(\gamma - 2)k + 2]\,N\}!}{M!}\right]^{\gamma/2}. \tag{22}$$

From Eq. (22), the canonical partition function $Q(M, N, T)$ can be easily calculated. Thus,

$$Q(M, N, T) = \Omega(M, N, \gamma)\exp(-\beta k\epsilon_o N) \tag{23}$$

where ϵ_o is the interaction energy between every unit forming a k-mer and the substrate. In addition, the Helmholtz free energy $F(M, N, T)$ relates to $\Omega(M, N, \gamma)$ through

$$\beta F(M, N, T) = -\ln Q(M, N, T) = -\ln\Omega(M, N, \gamma) + \beta k\epsilon_o N. \tag{24}$$

Then, the remaining thermodynamic functions can be obtained from the general differential form [26]

$$dF = -S dT - \Pi dM + \mu dN \tag{25}$$

where S, Π and μ designate the entropy, spreading pressure and chemical potential respectively, which, by definition, are

$$S = -\left(\frac{\partial F}{\partial T}\right)_{M,N} \qquad \Pi = -\left(\frac{\partial F}{\partial M}\right)_{T,N} \qquad \mu = \left(\frac{\partial F}{\partial N}\right)_{T,M}. \tag{26}$$

Finally, from Eqs. (22)–(26) and by using the lattice coverage $\theta = kN/M$, configurational entropy per site ($s = S/M$) and adsorption isotherm can be written in terms of the intensive variables θ and T.

$$\frac{s(\theta, \gamma)}{k_B} = \left[\frac{\gamma}{2} - \frac{(k-1)}{k}\theta\right]\ln\left[\frac{\gamma}{2} - \frac{(k-1)}{k}\theta\right] - \frac{\theta}{k}\ln\frac{\theta}{k} - (1-\theta)\ln(1-\theta) + \left(\theta - \frac{\gamma}{2}\right)\ln\frac{\gamma}{2} \tag{27}$$

$$\beta(\mu - k\epsilon_o) = \ln\left(\frac{\theta}{k}\right) - k\ln(1-\theta) - \ln\left(\frac{\gamma}{2}\right) + (k-1)\ln\left[1 - \frac{(k-1)}{k}\frac{2\theta}{\gamma}\right]. \tag{28}$$

Appendix B. Exact thermodynamic functions in one dimension and extension to higher dimensions

In this section, we address the calculation of approximated thermodynamical functions of chains adsorbed on lattices with connectivity γ higher than 2 (i.e. dimensions higher than one).

In general, the number of configurations of N k-mers on M sites, $\Omega(M, N, \gamma)$, depends on the lattice connectivity γ. $\Omega(M, N, \gamma)$ can be approximated considering that the molecules are distributed completely at random on the lattice, and assuming the arguments given by different authors [26–28] to relate the configurational factor $\Omega(M, N, \gamma)$ for any γ with respect to the same quantity in one dimension ($\gamma = 2$). Thus

$$\Omega(M, N, \gamma) = K(\gamma, k)^N \Omega(M, N, 2) \tag{29}$$

where $K(\gamma, k)$ represents the number of available configurations (per lattice site) for a k-mer at zero coverage. $K(\gamma, k)$ is, in general, a function of the connectivity and the size/shape of the adsorbate. It is easy demonstrate that,

$$K(\gamma, k) = \begin{cases} \gamma/2 & \text{for linear } k\text{-mers} \\ \left[\gamma(\gamma-1)^{(k-2)}\right]/2 - m' & \text{for flexible } k\text{-mers} \end{cases} \tag{30}$$

the term m' is subtracted in Eq. (30) since the first term overestimates $K(\gamma, k)$ by including m' configurations providing overlaps in the k-mer.

On the other hand, $\Omega(M, N, 2)$ can be exactly calculated as the total number of permutations of the N indistinguishable k-mers out of n_e entities, being n_e [15]

$$\begin{aligned} n_e &= \text{number of } k\text{-mers} + \text{number of empty sites} \\ &= N + M - kN = M - (k-1)N. \end{aligned} \tag{31}$$

Accordingly,

$$\Omega(M, N, 2) = \binom{n_e}{N} = \frac{[M - (k-1)N]!}{N![M - kN]!}. \tag{32}$$

By operating as in previous appendix, configurational entropy per site and adsorption isotherm of straight linear k-mers can be obtained from Eqs. (29)–(32)

$$\frac{s(\theta, \gamma)}{k_B} = \left[1 - \frac{(k-1)}{k}\theta\right] \ln\left[1 - \frac{(k-1)}{k}\theta\right] - \frac{\theta}{k}\ln\frac{\theta}{k} - (1-\theta)\ln(1-\theta) + \frac{\theta}{k}\ln\frac{\gamma}{2} \tag{33}$$

$$\beta(\mu - k\epsilon_o) = \ln\left(\frac{\theta}{k}\right) - k\ln(1-\theta) - \ln\left(\frac{\gamma}{2}\right) + (k-1)\ln\left[1 - \frac{(k-1)\theta}{k}\right]. \tag{34}$$

Appendix C. Semiempirical model for adsorption of polyatomics

Here, we propose an approximation of the adsorption isotherm for non-interacting linear k-mers on a regular lattice, based on semi-empirical arguments, which leads to very accurate results.

The mean number of particles in the adlayer $\bar{N}$ and the chemical potential μ are related through the following general relationship in the grand canonical ensemble

$$\bar{N} = \lambda\left[\frac{\partial \ln \Xi(M, \lambda)}{\partial\lambda}\right]_M \tag{35}$$

where $\lambda = \exp[\beta(\mu - k\epsilon_o)]$ and Ξ is the grand partition function. By solving λ^{-1} from Eq. (35)

$$\lambda^{-1} = \frac{1}{\bar{N}}\left[\frac{\partial \ln \Xi(M, \lambda)}{\partial\lambda}\right]_M = \frac{R(M, \lambda)}{\bar{N}}. \tag{36}$$

In the last equation, which is called Occupation Balance [29], the mean number of states available to a particle on M sites at λ, $R(M, \lambda)$, can be written as,

$$R = \left(\frac{\gamma}{2}M\right)\prod_{i=1}^{k} P_i \tag{37}$$

being γ the connectivity of the lattice. Eq. (37) can be interpreted as follows. The term between parentheses corresponds to the total number of k-uples on the surface. These k-uples can be separated in three groups: full k-uples (occupied by k-mers), empty k-uples (available for adsorption) and frustrated k-uples (partially occupied or occupied by segments belonging to different adsorbed k-mers). Then, an additional factor must be incorporated, which takes into account the probability of

having a empty k-uple. We suppose that this factor can be written as a product of k functions (P_i's), being P_i the conditional probability of finding the ith empty site into the lattice with $i-1$ already vacant sites (the i sites are assumed to be arranged in a linear k-uple). In the particular case of $i=1$,

$$P_1 = 1-\theta. \tag{38}$$

Eq. (38) represents an exact result.

Now, let us consider the simplest approximation within this scheme, namely, $P_i = P_1$ for all i. Then, from Eqs. (36)–(38) result,

$$\lambda^{-1} = \frac{R}{\bar{N}} = \frac{\gamma k}{2}\frac{M}{k\bar{N}}{P_1}^k = \frac{\gamma k(1-\theta)^k}{2\theta} \tag{39}$$

or

$$\beta\,(\mu - k\epsilon_o) = \ln\left(\frac{\theta}{k}\right) - k\ln(1-\theta) - \ln\left(\frac{\gamma}{2}\right). \tag{40}$$

Eq. (40) reduces to the well-known Flory–Huggins isotherm of non-interacting linear k-mers adsorbed flat on homogeneous surfaces [27,30]. This is already a simple example out of a whole variety of multisite adsorption models that the proposed formalism allows to deal with.

In general, the P_i's can be written as

$$P_i = (1-\theta)C_i, \tag{41}$$

where a correction factor, C_i, has been included (being $C_1 = 1$ and $C_i \to 1$ as $\theta \to 0$). From Eqs. (37)–(41), we obtain

$$R = \frac{\gamma}{2}M(1-\theta)^k\prod_{i=2}^{k}C_i = \frac{\gamma}{2}M(1-\theta)^k\tilde{C}^{k-1} \tag{42}$$

and

$$\tilde{C} = \left(\prod_{i=2}^{k}C_i\right)^{\frac{1}{k-1}} \tag{43}$$

being $\tilde{C}$ the average correction function, which is calculated as the geometrical mean of the C_i's. Then, from Eqs. (36) and (42), the general form of the adsorption isotherm can be obtained:

$$\lambda^{-1} = \frac{\gamma k(1-\theta)^k\tilde{C}^{k-1}}{2\theta} \tag{44}$$

or

$$\beta\,(\mu - k\epsilon_o) = \ln\left(\frac{\theta}{k}\right) - k\ln(1-\theta) - \ln\left(\frac{\gamma}{2}\right) - (k-1)\ln\tilde{C}. \tag{45}$$

It is interesting to compare Eq. (45) with corresponding ones obtained from the main theories of adsorption of polyatomics. As it can be observed, Eqs. (28), (34) and (40) have the structure of Eq. (45). From this new perspective, the differences between the theoretical models arise from the distinct strategies of approximating $\tilde{C}$. These arguments can be better understood with an example: Eqs. (28) and (34) provide the exact solution for the one-dimensional case. Then, the comparison between Eq. (45) and the adsorption isotherm from Eq. (34) (or Eq. (28) with $\gamma = 2$) allows us to obtain:

$$\tilde{C}^{-1} = 1 - \frac{k-1}{k}\theta \qquad (\gamma = 2). \tag{46}$$

The result in Eq. (46) is exact. Moreover, it can be demonstrated that $C_i = \tilde{C}$ for all i [21].

Then, it is clear that the differences between Eqs. (28) and (34) can be only associated to the average correction function $\tilde{C}$. In addition, detailed comparisons between theoretical and simulation results of adsorption [22] shown that Eq. (28) fits the numerical data very well at low coverage, while the Eq. (34) behaves excellently at high coverage. These findings, along with the structure proposed for the adsorption isotherm [Eq. (45)], allow us to build a new semiempirical adsorption isotherm for polyatomics,

$$\begin{aligned}\beta\,(\mu - k\epsilon_o) = {} & \ln\left(\frac{\theta}{k}\right) - k\ln(1-\theta) - \ln\left(\frac{\gamma}{2}\right) + (1-\theta)(k-1)\ln\left[1 - \frac{(k-1)}{k}\frac{2\theta}{\gamma}\right] \\ & + \theta(k-1)\ln\left[1 - \frac{(k-1)\theta}{k}\right].\end{aligned} \tag{47}$$

The last equation can be interpreted as follows. The first line includes three terms, which are identical in both Eqs. (28) and (34). The second and third lines represent a combination of the average correction functions corresponding to Eqs. (28) and (34), with $(1-\theta)$ and θ as weights, respectively. The corresponding configurational entropy per site is given by

$$\begin{aligned}\frac{s(\theta,\gamma)}{k_B} &= -\frac{\theta}{k}\ln\frac{\theta}{k} - (1-\theta)\ln(1-\theta) + \theta\left[\frac{1}{2} - \frac{\gamma}{4} + \frac{1}{k}\ln\left(\frac{\gamma}{2}\right)\right] \\ &\quad + \frac{1}{2}\frac{k}{(k-1)}\left[1 - \frac{(k-1)^2}{k^2}\theta^2\right]\ln\left[1 - \frac{(k-1)}{k}\theta\right] \\ &\quad - \frac{\gamma}{4}\left[\theta + \frac{k(\gamma-4)+4}{2(k-1)}\right]\left[1 - \frac{2(k-1)}{\gamma k}\theta\right]\ln\left[1 - \frac{2(k-1)}{\gamma k}\theta\right]. \end{aligned} \tag{48}$$

References

[1] D.A. Matoz-Fernandez, D.H. Linares, A.J. Ramirez-Pastor, Europhys. Lett. 82 (2008) 50007.
[2] D.H. Linares, F. Romá, A.J. Ramirez-Pastor, J. Stat. Mech. (2008) P03013.
[3] D.A. Matoz-Fernandez, D.H. Linares, A.J. Ramirez-Pastor, J. Chem. Phys. 128 (2008) 214902.
[4] K. Binder, Applications of the Monte Carlo Method in Statistical Physics, in: Topics in Current Physics, vol. 36, Springer, Berlin, 1984.
[5] A. Ghosh, D. Dhar, Eur. Phys. Lett. 78 (2007) 20003.
[6] F.Y. Wu, Rev. Modern. Phys. 54 (1982) 235.
[7] J.E. González, A.J. Ramirez-Pastor, V.D. Pereyra, Langmuir 17 (2001) 6974.
[8] F. Romá, J.L. Riccardo, A.J. Ramirez-Pastor, Langmuir 21 (2005) 2454.
[9] M. Dávila, F. Romá, J.L. Riccardo, A.J. Ramirez-Pastor, Surf. Sci. 600 (2006) 2011.
[10] P.M. Pasinetti, J.L. Riccardo, A.J. Ramirez-Pastor, Physica A 355 (2005) 383.
[11] J.P. Hansen, L. Verlet, Phys. Rev. 184 (1969) 151.
[12] K. Binder, J. Stat. Phys. 24 (1981) 69.
[13] K. Binder, Z. Phys. B 45 (1981) 61.
[14] T.L. Polgreen, Phys. Rev. B 29 (1984) 1468.
[15] A.J. Ramirez-Pastor, T.P. Eggarter, V.D. Pereyra, J.L. Riccardo, Phys. Rev. B 59 (1999) 11027.
[16] V. Privman, Finite Size Scaling and Numerical Simulation of Statistical Systems, World Scientific, Singapore, 1990.
[17] T. Tomé, A. Petri, J. Phys. A 35 (2002) 5379.
[18] W. Selke, L.N. Shchur, J. Phys. A 38 (2005) L739.
[19] W. Selke, J. Stat. Phys. (2007) P04008.
[20] E.A. Guggenheim, Proc. R. Soc. Lond. A183 (1944) 203.
[21] E.A. DiMarzio, J. Chem. Phys. 35 (1961) 658.
[22] F. Romá, J.L. Riccardo, A.J. Ramirez-Pastor, Langmuir 22 (2006) 3192.
[23] A.M. Ferrenberg, D.P. Landau, Phys. Rev. B 44 (1991) 5081.
[24] W. Janke, M. Katoot, R. Villanova, Phys. Rev. B 49 (1994) 9644.
[25] F. Nieto, V. Pereyra, Surf. Sci. 399 (1998) 96.
[26] T.L. Hill, An Introduction to Statistical Thermodynamics, Addison Wesley Publishing Company, Reading, MA, 1960.
[27] P. Flory, J. Chem. Phys. 10 (1942) 51; Principles of Polymer Chemistry, Cornell, Ithaca, NY, 1953.
[28] J. Des Cloizeaux, G. Jannink, Polymers in Solution. Their Modelling and Structure, Clarendon, Oxford, 1990.
[29] F. Romá, A.J. Ramirez-Pastor, J.L. Riccardo, Langmuir 19 (2003) 6770.
[30] M.L. Huggins, J. Chem. Phys. 46 (1942) 151; Ann. New York Acad. Sci. 41 (1942) 151; J. Am. Chem. Soc. 64 (1942) 1712.